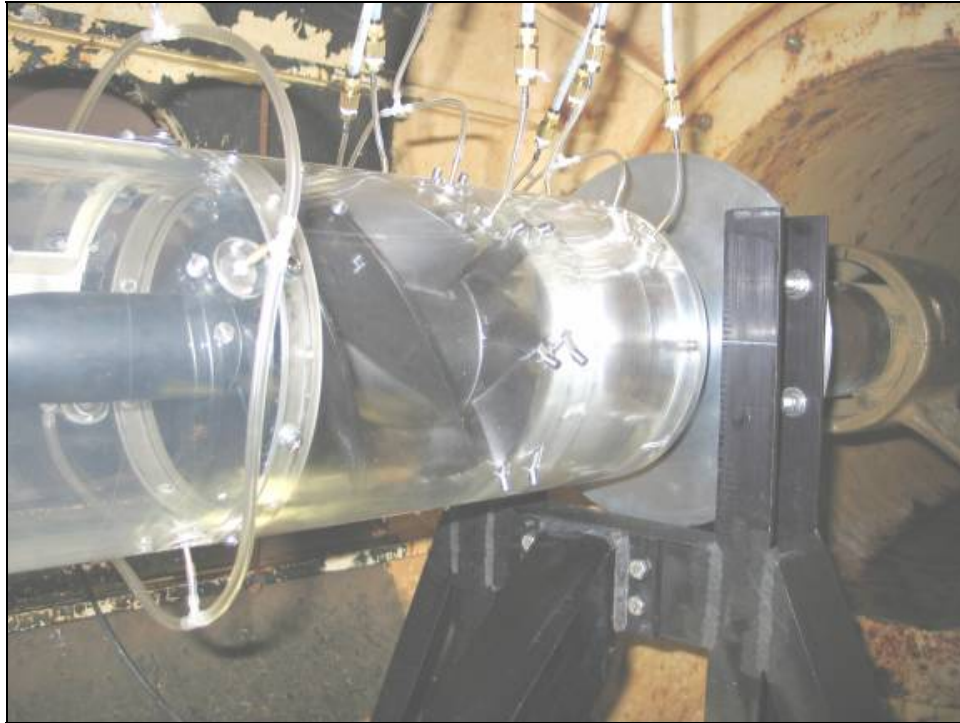


# ADVANCED COMPACT WATERJET PROPULSION FOR HIGH-SPEED SHIPS

David R. Lavis<sup>1</sup>, Brian G. Forstell<sup>1</sup> and John G. Purnell<sup>1</sup>



## ABSTRACT

*The paper describes the development and validation of a compact waterjet propulsion system for high-speed vessels. The development was conducted in four discrete phases: 1) Comparison of Waterjet Types, 2) Pump Detail Design & Sealift Ship Concept Design, 3) Cavitation Tunnel Model Tests, and 4) Self-Propulsion Model Tests. The focus of the paper is on phases 2 and 3.*

## KEY WORDS

Waterjet; Propulsion; High-Speed Vessels; Computational Fluid Dynamics; Cavitation; Model; Tests

---

<sup>1</sup> CDI Marine Systems Development Division (CDIM-SDD) (formerly Band, Lavis & Associates, Inc.)

## NOMENCLATURE

<u>Symbol</u>	<u>Definition</u>	<u>Units</u>
CFD	Computational Fluid Dynamics	--
D	Impeller or Duct Diameter	ft
g	Gravitational Constant	ft/sec <sup>2</sup>
GPM	Gallons per Minute	gal/min
H	Headrise	ft
H <sub>tot</sub>	Pump Total Headrise	ft
H <sub>0</sub>	Initial Headrise	ft
IVR	Inlet Velocity Ratio	--
JVR	Jet Velocity Ratio	--
K <sub>ram</sub>	Ram Recovery	--
LDV	Laser Doppler Velocimeter	--
NPSH	Net Positive Suction Head	--
N <sub>ss</sub>	Suction Specific Speed	--
Q	Volume Flow Rate	ft <sup>3</sup> /sec
Q <sub>d</sub>	Design Point Volume Flow Rate at Design RPM	ft <sup>3</sup> /sec
RPM	Shaft Rotational Speed	revs/sec
SHP	Shaft Horsepower	horsepower
U <sub>TIP</sub>	Impeller Tip Velocity	ft/sec
V <sub>axial</sub>	Axial Inflow Velocity	ft/sec
V <sub>o</sub>	Craft Velocity	knots
φ	Flow Coefficient (Phi)	V <sub>axial</sub> / U <sub>TIP</sub>
ψ <sub>tip</sub>	Pump Head Coefficient	2gH <sub>tot</sub> / U <sub>TIP</sub> <sup>2</sup>

## INTRODUCTION

High-ship speeds generally require the use of slender hullforms (to reduce the ship's wave drag) and efficient, but compact, propulsion systems (to minimize the total installed power and installation space required). For this application, waterjets are often a preferred choice since:

- they have no appendage drag (with a flush-mounted waterjet inlet); and
- they have high efficiency (because they recover part of the ship's frictional drag by ingesting the low momentum boundary layer at the waterjet inlet).

However, today's commercially available large waterjets, above 10,000 horsepower, are large mixed-flow pumps. For these pumps, the installation flange diameter is 70 to 85 percent larger than the diameter of the inlet flow duct, and this large flange diameter is often incompatible with the slender hulls required for high-speed ships. Increasing the hull's beam to accommodate the size and number of mixed-flow waterjets required could result in significant increases in drag, which leads to a spiraling increase in ship displacement and the power that must be installed. Axial-flow waterjet pumps, however, have installation flange diameters that are only about 15 to 20 percent larger than the inlet duct and, since they are also much lighter in weight, they are a potential solution to this problem.

Thus, in 2002, The Center for Commercial Deployment of Transportation Technologies (CCDoTT) of California State University at Long Beach funded CDIM-SDD for a four-year program to examine technology options and eventually to focus on the RDT&E to develop and validate compact axial-flow pumps, as illustrated in Figures 1, 2 and 3.

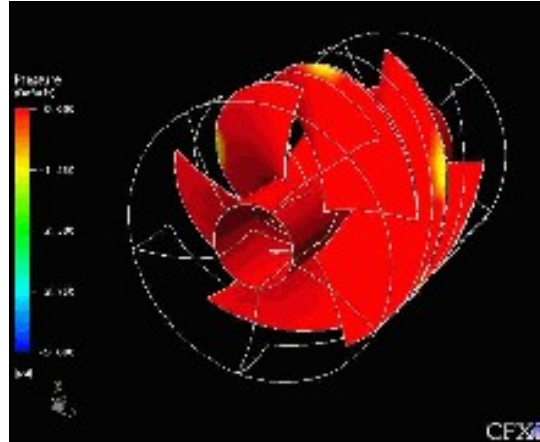


**Figure 1: Pump & Ship Design, Phases 1 and 2**

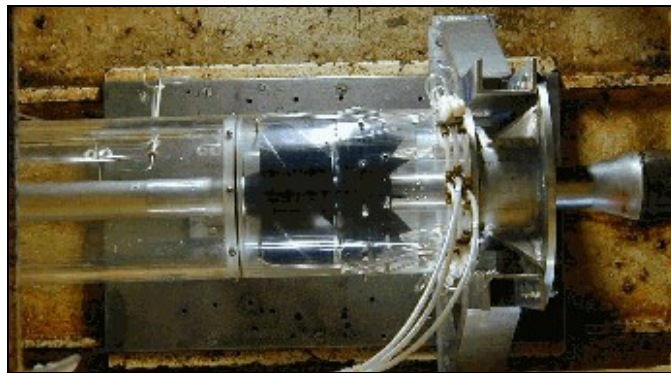


**Figure 2: Cavitation Test, Phase 3**



**Figure 3: Self-Propulsion Tests, Phase 4**

The objective of this four-phase project for CCDoTT is to develop and validate the attributes of a preferred compact waterjet propulsor suitable for high-speed sealift applications where waterjet propulsion is the only realistic choice. The four phases of the project are:

- Phase 1: Exploration and Comparison of Waterjet Propulsion System Types, completed Aug. 02
- Phase 2: Concept Design of Sealift Ship and Propulsion System, completed Sept. 03
- Phase 3: Cavitation Tunnel Tests, completed July 05
- Phase 4: Self-Propulsion Tests, completion due July 06

This paper focuses on describing the approach to phases 2 and 3, with the other two phases summarized in context below:

Phase 1 of the four-phase project studied options for compact units, including the following:

- 1) Pumps with Contra-Rotating Blade Rows,
- 2) Pumps with Inlet Pre-Swirl Vanes,
- 3) Ventilated Pumps,
- 4) Super-Cavitating Pumps, and
- 5) Axial-Flow Pumps.

The latter was chosen for further work.

Phase 2 developed the concept design of a waterjet-propelled, 50-knot, 600-ft long slender monohull RO/RO ship for commercial coastal short-sea shipping. This design was developed with help from the CDIM-SDD whole-ship design synthesis model PASS<sup>TM</sup>, which helped to confirm the choice of axial waterjet pumps as having the most favorable ship impact to minimize ship fuel consumption and maximize overall ship economy of operation.

Phase 3 involved the Computational Fluid Dynamic (CFD) analysis, manufacture, and tunnel testing of a model waterjet pump that was required to adequately validate the pump's critical powering characteristics and cavitation limits.

Phase 4 involves the construction and testing, in a towing tank, of a suitable high-speed model for, among other things, the critical interaction effects between the hull and the waterjet inlet. It determines the pump's powering characteristics at design point and off-design operating conditions. Data developed will cover the full range of ship operating conditions anticipated for the primary full-scale waterjet propulsor. Testing utilizes a Laser Doppler Velocimeter (LDV) system to characterize and define the flow-fields and assure performance prediction accuracy.

The whole-ship and ship interaction data, combined with pump model tests of Phase 3, will provide the critical information necessary to validate the design process and the CFD modeling process. This will enable realization of the Overall Project Goal: To enable the realistic design and prediction of overall full-scale performance of large (>40 MW) axial-flow pumps in a high-speed ship application using the proper and appropriate model testing and data scaling procedures such as those defined by the International Towing Tank Conference (ITTC).

It should be realized that axial-flow waterjet pumps are not new, as they have been in serious use in various forms for several hundred years (Allison 1992). The type of axial-flow pump selected for this current application has its roots in separate work performed originally by Aerojet General Corporation and by Rocketdyne in the U.S. in support of various U.S. hydrofoil and SES programs in the 1960's and 70's, which were subsequently discontinued. However, starting in 1987, Band, Lavis & Associates (now CDI Marine Systems Development Division (CDIM-SDD)) picked up the thread and began further development that has now resulted in numerous pump model tests for the world's leading waterjet manufacturers and installation on several craft, including the U.S. Marine Corps Expeditionary Fighting Vehicle (EFV) (formerly the AAV) high-speed tracked amphibian. The work reported in this paper is the most recent effort in this evolution with a focus on establishing a set of notional requirements based on the concept design of a high-speed commercial RO/RO ship and the detail design of a pump for this ship, followed by performance and cavitation tests in a closed circuit tunnel conducted in 2005 and self-propelled model towing tank tests that are due to be conducted in 2006. As mentioned previously, the sponsorship of this 4-year program of work was provided by CCDoTT, but with oversight by the Office of Naval Research (ONR) and support from the Naval Surface Warfare Center (NSWC) Carderock Division and the Marine Propulsors Company, Berlin, MD.

## SHIP DESIGN AND WATERJET PUMP REQUIREMENTS

The need for high speed, i.e. speeds of 45 to 50 knots and beyond, will require the use of slender hullforms and efficient propulsion systems in order to reduce the ship's wave drag and, therefore, the required installed power. Since drag typically increases on the order of the square or higher of the ship speed, low-drag slender hulls will be a necessity. But slender hulls introduce a problem of installing the necessary machinery to achieve high speed. A conventional external propeller arrangement with its exposed shaft, shaft supports, and rudder has significant appendage drag that eliminates it from consideration for most high-speed applications. In addition, the external propeller impacts any desired hull shape by requiring trade-offs and modifications to accommodate its presence. Above the 25 to 35 knots speed range, waterjet propulsion has been increasingly the propulsion system of choice.

The conflicting high-speed requirements of slender hulls and large amounts of installed power with multiple waterjets has led to the need for a trade-off study to determine the best hullform and propulsion machinery arrangement for high-speed sealift ships and a development program to design high-power density axial-flow waterjets.

Prior to conducting the hullform trade-off analysis, a review of the results from the CDNSWC High-Speed Sealift Technology Development Plan of NSWCCD-20-TR-2002/06 was conducted to select a mission for the development of an advanced axial-flow waterjet. Table 1 is a mission summary from the technology development plan. The technology development plan identified 15 different missions and grouped them into current, near-term (available in 5 years), and far-term (available in 10 years) missions based on the technologies required to meet the mission goals. The commercial coastal mission was chosen after reviewing the 15 missions since it represents the current state-of-the-art in terms of available gas turbines and structural technology. The coastal commercial ship mission requirements are a top speed of 50 knots, with a payload of 1500 metric tons, and a range of 1500 nautical miles in a 2.4-meter wave height. The required manning for this mission is a crew of 20. The waterjet technology should be stated as near-term and not current since this mission will require waterjets larger than any previously built. The largest waterjet in current operation has an inlet diameter of about 6.9 feet at a horsepower of about 35,000. The coastal commercial mission will require waterjets larger than this size, with power levels on the order of 57,000 to 67,000 horsepower per gas turbine if the number of gas turbines is to be kept to a reasonable number. This mission represents the next step beyond the current state-of-the-art in waterjet technology development. At a 50-knot top speed, this mission also represents current U.S. Navy requirements for high-speed small combatants, so waterjets developed for the coastal commercial mission could be geometrically scaled to meet other similar high-speed mission requirements.

**TABLE 1: MISSION SUMMARY**

	Shuttle Ship 1a	Shuttle Ship 1b	Intra-Theater Support Ship 2a	Intra-Theater Support Ship 2b	Coastal Commercial Ship 3	Trans-Ocean Commercial Ship 4a	Trans-Ocean Commercial Ship 4b	Inter-Theater Ship 5
Average Speed (knots)	40	45	40	40	50	50	60	40
Full Performance Wave Height (m)	2.4	2.4	2.4	2.4	2.4	4	4	4
Range (nm)	1,250	1,250	800	1,200	1,500	4,000	4,000	5,000
Payload (mt)	1,497	1,497	454	454	1,500	7,500	7,500	5,445
Ramp Requirements	y	y	y	y	n	n	n	y
Total Crew	20	20	20	20	20	30	30	30
Structural Technology	current	current	current	current	current	far	far	near
Waterjet Technology	current	current	current	current	current	far	far	near
Prime Mover Technology	current	current	current	current	current	far	far	near

	Vision Ship 70 knots 6a	Vision Ship 60 knots 6b	Vision Ship 55 knots 6c	Vision Ship 5,000 st 7a	Vision Ship 7,500 st 7b	Intra-theater Ship 8	Logistics Ship 9
Average Speed (knots)	70	60	55	55	55	40	50
Full Performance Wave Height (m)	4	4	4	4	4	2.4	2.4
Range (nm)	5,000	5,000	10,000	8,700	8,700	800	1,000
Payload (mt)	4,537	11,797	11,797	4,537	6,806	1,312	726
Ramp Requirements	y	y	y	y	y	y	y
Total Crew	30	30	30	30	30	20	20
Structural Technology	far	far	far	far	far	near	near
Waterjet Technology	far	far	far	far	far	near	near
Prime Mover Technology	far	far	far	far	far	near	near

The trade-off study was conducted using CDIM-SDD's PASS<sup>TM</sup> whole-ship design simulation software that allows a broad range of ship parameters to be varied systematically to determine the optimum ship based on weight, acquisition cost, life-cycle cost or power. PASS<sup>TM</sup> follows the classical naval architecture design spiral, but, by automating the procedure, many design permutations can be investigated in a short time to arrive at the optimum design for a given mission. The software requires 13 groups of inputs to adequately define the ship and its mission profile. These input groups are Geometry, Structure, Propulsor, Propulsion Plant, Electrical Plant, Command and Surveillance, Auxiliaries, Outfit and Furnishings, Armament, Payload, Margins and Standards, Performance, and Cost. The software calculates a balanced design for each set of inputs; therefore, the effect of changing one input, while holding all others constant, can be accessed on the overall ship design. This procedure was used for the trade-off study so that, once the inputs were set for a given hull type, the only variable that was changed was the type of waterjet. The two types of waterjets used were the advanced axial-flow and commercial mixed-flow waterjets. These two types of waterjets were evaluated in four different hullforms; a monohull, a catamaran, a trimaran, and a SES, to determine the optimum arrangement for a coastal commercial mission.

The monohull variant for the coastal commercial mission was modeled in PASS<sup>TM</sup> with a variety of propulsion machinery arrangements to determine the optimum layout. The number of gas turbines and waterjets was varied from three to five, and the relative power levels were varied between the main and auxiliary engines. All systems included steering only on the two outermost waterjets, with the others acting as booster jets. After making many runs of PASS<sup>TM</sup>, it was determined that the optimum arrangement was four gas turbines of the same power driving four waterjets of the same size. Table 2 shows a summary of the results for the axial-flow propelled monohull with three, four and five waterjets. The three-gas-turbine arrangement resulted in a center gas turbine with a power level greater than 125,000 horsepower. These gas turbines are not currently available. Also, the center waterjet, with an inlet diameter of 8.8 feet, was larger than the four-gas-turbine arrangement waterjets. The total displacement, total absorbed power, and life-cycle cost were also much higher. The five-waterjet arrangement resulted in smaller waterjets, but the installed power and life-cycle costs were much higher than the four-waterjet arrangement. The arrangement of four similar gas turbines driving four waterjets of the same size, with steering on the two outer jets, was the best configuration for this mission and was used for all hull types investigated in this study.

**TABLE 2: PASS™ MONOHULL RESULTS WITH WATERJET VARIATION**

Water Type/Number	Length (ft)	Beam (ft)	Draft (ft)	Displacement (LT)	Installed Power (hp)	Absorbed Power (hp)	Waterjet Inlet Diameter (ft)	Waterjet Installation Diameter (ft)	LLC/hr (\$/hr)
Axial 3 WJs	600	54.55	20.3	8,676	263,963	232,851	8.8/7.2	11.0/9.0	19,176
Axial 4 WJs	600	54.55	19.6	8,376	229,320	215,993	7.2	9.0	17,321
Axial 5 WJs	600	54.55	19.9	8,432	268,510	225,472	5.8	7.25	18,956

Figure 4 shows the results of the PASS™ run for the axial-flow waterjet-propelled monohull, where the length varied from 500 to 700 feet, the length-to-beam varied from 9 to 13, and the block coefficient was held constant at 0.45. The length and length-to-beam are plotted versus the displacement, with this surface colored by life-cycle cost per hour. A contour of constant beam-to-draft equal to 2.5 is shown on Figure 4 for reference. A beam-to-draft of 2.5 or greater is required for good seakeeping performance for a monohull, so designs below this value were eliminated from consideration.

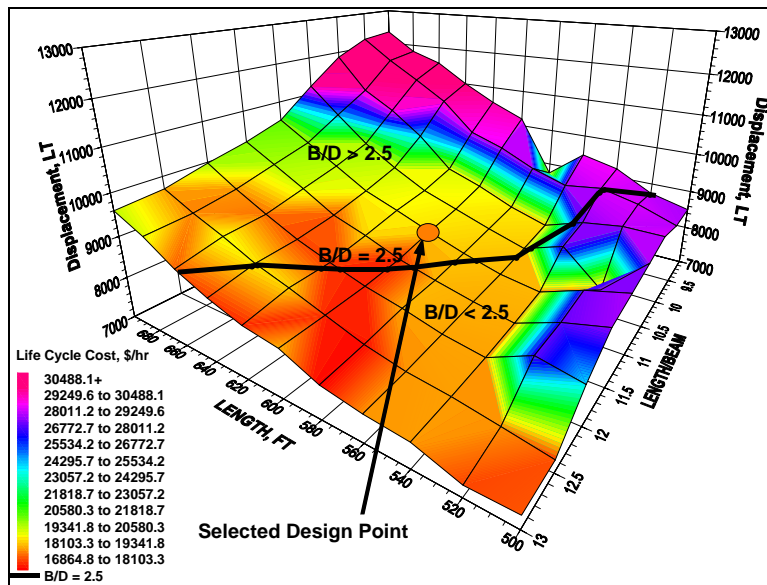


**Figure 4: PASS™ Results for Monohull with Axial-Flow Waterjet**

In reviewing Figure 4, it is seen that the monohull results from the PASS™ analysis determined that the optimum ship length was 600 feet at a length-to-beam ratio of 11 for the advanced axial-flow waterjet. The total displacement was 8376 long tons with four General Electric LM6000's driving four 7.2-foot diameter waterjets. The total installed power was 229,320 horsepower, with 215,993 horsepower absorbed at top speed, and the life-cycle cost per hour was 17,312 dollars.

This ship design point was used as the basis for setting the design requirements of the axial-flow pumps that are described in the next chapter of this paper.

## WATERJET PROPULSION SYSTEM DESIGN

The basic application that was examined was a large, high-power, axial-flow waterjet designed for a 50-knot sealift application. However, the design is not limited to this application design point, but can be scaled to other speeds and powers through appropriate application of the scaling laws for the design. Based on the desired waterjet system requirements, initial sizing and performance estimates for an axial-flow waterjet system can be made using basic

pump design theory combined with empirical correlations to account for cavitation limits, waterjet system pressure losses, etc. Review of this data is important in that it will establish the diameter, rpm, flow rate, and headrise objectives for the pump design that meets the thrust and powering requirements in an optimum manner. This provides a physical envelope within which to accomplish the design and the performance requirements to initialize the design. The prototype axial-flow waterjet pump design point parameters were established based on an initially conservative 90 percent overall pump hydraulic efficiency. As shown later, this value was subsequently calculated as a somewhat larger value. For 90%, however, the design point parameters were as follows:

Impeller diameter:	90 in
Nozzle diameter:	58.4 in
Maximum power:	57,330 SHP
Shaft speed:	406.9 RPM
Flow rate:	2405.9 cfs
Headrise:	184.2 ft seawater
Suction specific speed:	15,005 (maximum value)

The actual design of the axial-flow waterjet, and particularly its blading to meet the requirements, is heavily dependent on the use of Computational Fluid Dynamics (CFD). CFD does not design the pump, but tells one how a design will perform based on the detailed geometry and flow condition input for that particular design. The main item is to develop blade geometries, both for the rotor and the stator, that are close to design requirements and will be in sufficient geometric detail for easy use in the CFD to avoid extensive runs on unproductive designs.

## Pump Geometry

TURBOdesign<sup>-1</sup> was used to develop the detailed geometry of the rotor blades using the meridional geometry, radial loading distribution, and blade numbers based on the diffusion factor developed using the streamline curvature method. TURBOdesign<sup>-1</sup> is a potential-flow inverse method where the requirements for the rotor are inputs and the blade geometry is the output. TURBOdesign<sup>-1</sup> does not take into account the viscous effects, but these effects were modeled using the CFD Navier-Stokes solver ANSYS CFX. TURBOdesign<sup>-1</sup> and ANSYS CFX were used iteratively to arrive at the final optimized rotor blade geometry. The minimum blade number based on the diffusion factor for the rotor is five. The blade profile used was a modified C4 section with a 6.67 percent trailing edge thickness. The rotor hub axial length was 58.5 inches with a maximum normal blade thickness of 3.937 inches, and the tip axial length, which was leaned forward 1.75 inches, was 60.25 inches with a maximum normal blade thickness of 2 inches. The inlet flow was assumed to be uniform in the axial direction, and the total pressure used at the pump inlet face was 106.8 feet of seawater, which accounted for boundary layer capture effects and waterjet inlet losses. Figure 5 shows the 3-dimensional geometry with the blade surface static pressure distribution. Figure 6 shows the blade surface static pressure distribution on the leading edge suction side where the pressure would be the lowest. This shows that the minimum pressure is 21.56 kPa, or 7 feet of seawater above vapor pressure at the 50-knot top speed.



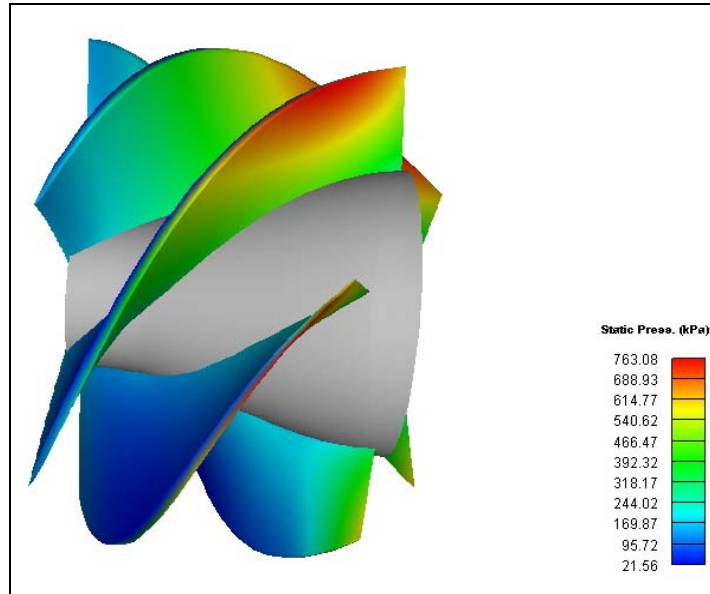


**Figure 5: Blade Surface Static Pressure Distribution for Waterjet Rotor**

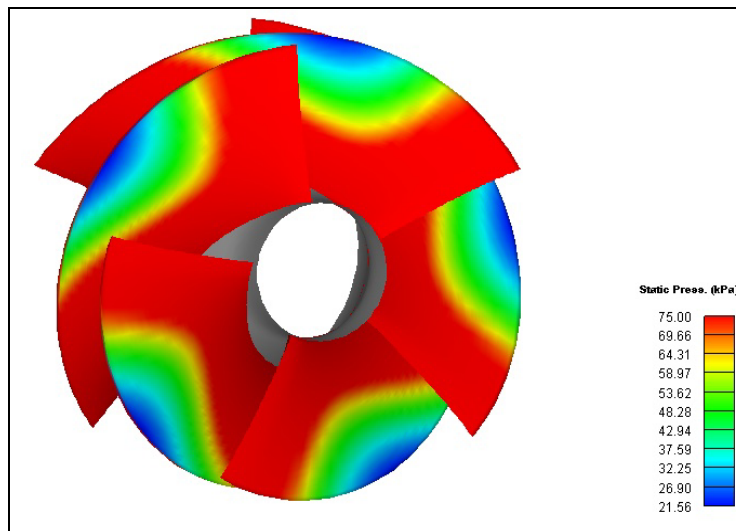


**Figure 6: Suction Side Leading Edge Static Pressure Distribution for Waterjet Rotor**

A linear stress analysis of the five-bladed waterjet rotor was conducted to verify structural strength and to ensure that blade deflections would not allow the tips of the blades to contact the casing shroud. Boundary conditions restricting translations were applied at the nodes corresponding to points on the hub. Loads applied included the pressure distribution on the blade, obtained from the TURBODesign<sup>1</sup> analysis, and centrifugal loads corresponding to a rotational speed of 406.9 RPM. The material properties used were for 15-5 stainless steel with a weight density of .284 pounds per cubic inch, Young's modulus of 28,500,000, and a Poisson ratio of 0.272. A contour plot depicting the deflections of one blade is shown in Figure 7. The maximum deflection seen by the blade is 0.069 inches and this occurs at the tip of the leading edge. The maximum radial deflection of the blade tip was found to be 0.006 inches, which is significantly less than the gap between the blade tip and housing. Figures 8 and 9 show the maximum and minimum principal stresses on the pressure and suction sides of the blade, respectively. The threshold values obtained of 15,871 psi and minus 14,221 psi are considerably less than the allowable values for 15-5 stainless steel. Both stresses occur at the root of the blade and can be further alleviated by fillets.

Stator blades were designed in the same manner and approach as the rotor blades, but used the output conditions of the rotor blades as their input. There were eight stator blades used in the design, and the outer diameter of the stator blades was decreased through the blade to allow a much shorter stator-nozzle section that will reduce the overall waterjet system weight. This type of blade design approach would be hard to evaluate without the use of CFD.

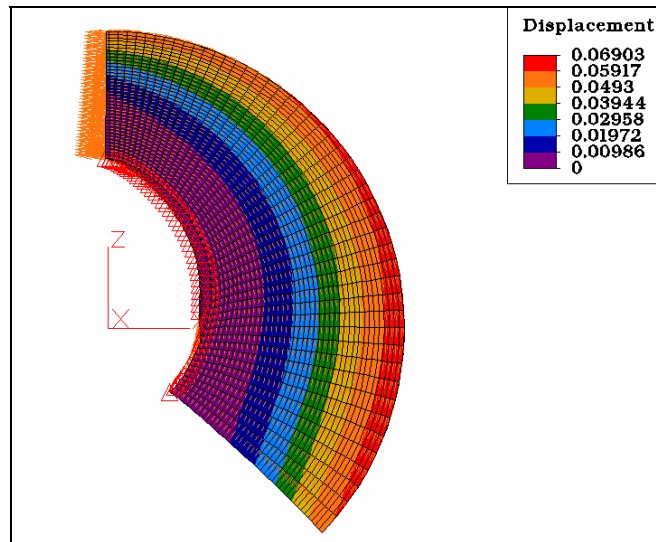


Figure 7: Contour Plot of Deflections for the Waterjet Rotor Blade (inches)

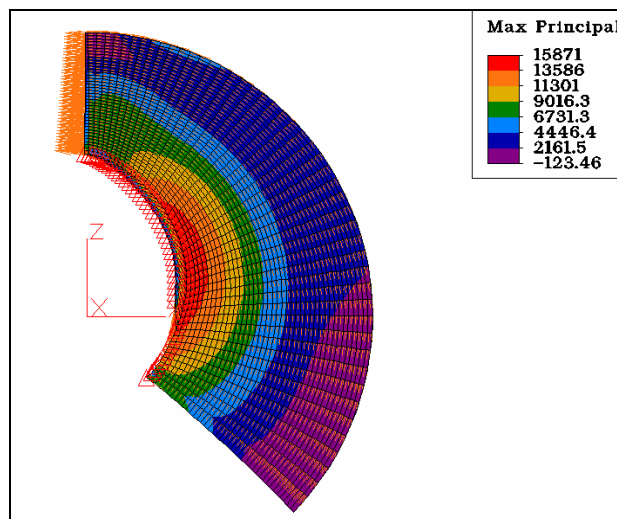
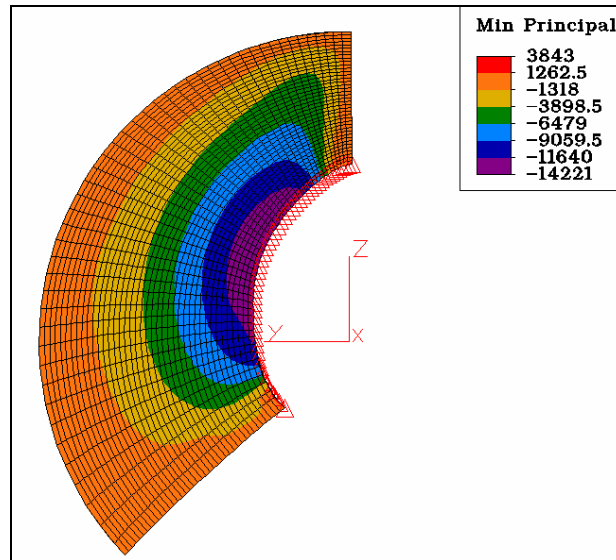


Figure 8: Contour Plot of Maximum Principal Stress for the Waterjet Rotor Blade (psi)



**Figure 9: Contour Plot of Minimum Principal Stress for the Waterjet Rotor Blade (psi)**

## Inlet Geometry

The waterjet inlet moves flow from outside the hull, through a flush-mounted inlet, and delivers it to the inlet face of the waterjet impeller. Because of its low drag features, the flush type inlet is the logical choice of inlet for most waterjet applications. With the flush inlet, the inlet flow will capture boundary layer flow from the hull region forward of the inlet as it meets the flow requirements of the waterjet impeller. Many variables affect the design of the waterjet inlet, such as flow rate, ship speed, local hull rake angle, nozzle elevation, inlet ramp angle, etc. The preferred inlet needs to capture and duct the flow to the waterjet impeller with a minimum of losses while providing a reasonably uniform flow velocity at the impeller face. Depending on the design requirements of the impeller, the waterjet inlet will need to be designed to change the flow velocity to match the required inlet flow velocity at the impeller face that is dictated by the design point. Two primary types of flush inlets are in use for waterjets. The shape of the opening that is made in the hull, which is either an elliptical or a rectangular inlet opening, basically classifies these, although combinations of the two are used. The merits of the two inlet types are the subject of debate, but, properly designed, either should provide comparable performance.

Since the inlet design will need to be modified frequently during the overall design process, it was necessary to develop an analytical approach that would allow the inlet design to be revised and updated in a timely manner as layout requirements in the hull and CFD computational results dictated. For this, a spreadsheet program was developed earlier to layout the centerline cut through a waterjet inlet using some basic geometric parameters. Figure 10 shows the resulting centerline cut. Basic inputs are the overall inlet length, the inlet diameter (which is the impeller inlet diameter), and a hull rocker angle. The inlet center depth is the vertical distance between the shaft centerline and the inlet ramp tangency point with the hull. When a hull rocker angle is included in the design, the inlet is laid out as though it has a smaller inlet center depth. In another computer program, which develops the inlet surfaces about the centerline profile, the centerline profile is rotated by the rocker angle, and a cylindrical wedge is added at the impeller inlet face of the inlet to match the rocker angle rotation and to give a vertical exit face for the inlet. Deadrise angle is included only if the inlet is located on the ship centerline, which would account for mounting the inlet in the middle of the V-shaped surface, which is not the case here. Keeping the centerline lip radius to reasonable values within a couple of percent of the inlet diameter is desirable. Too large a center lip radius will add drag, and too small or sharp a lip radius is more prone to cavitation. Since significant flow can come in on the sides of the inlet, a side edge radius is indicated in the inputs. The centerline lip radius is arranged to grow across the width of the inlet to match the side radius to ultimately define the entire lip surface. The spreadsheet program then calculates all the additional details of the inlet centerline layout, which are then updated and displayed with each variable change as shown in Figure 11.

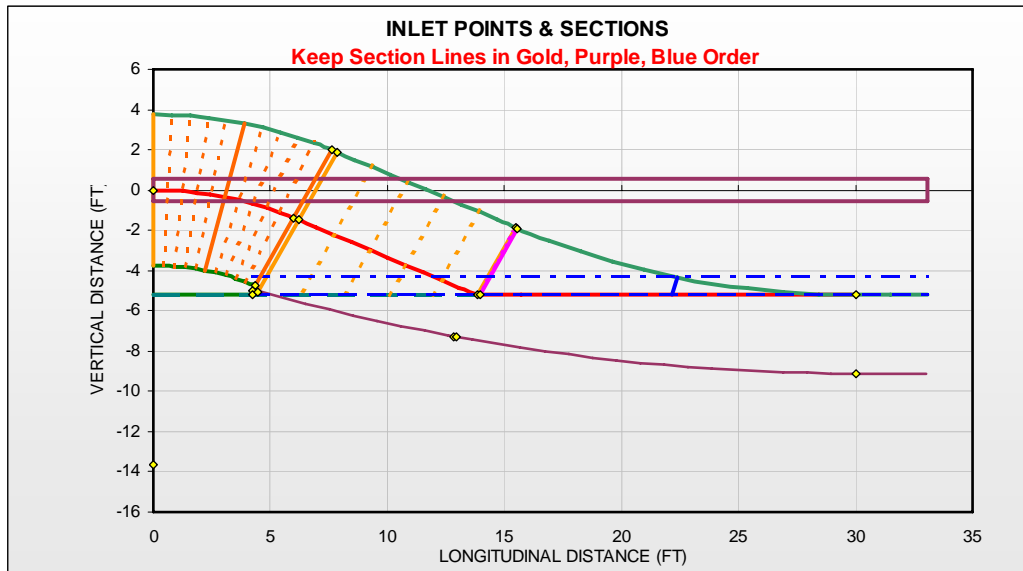


Figure 10: Waterjet Inlet Centerline Cut Design Program – Plot

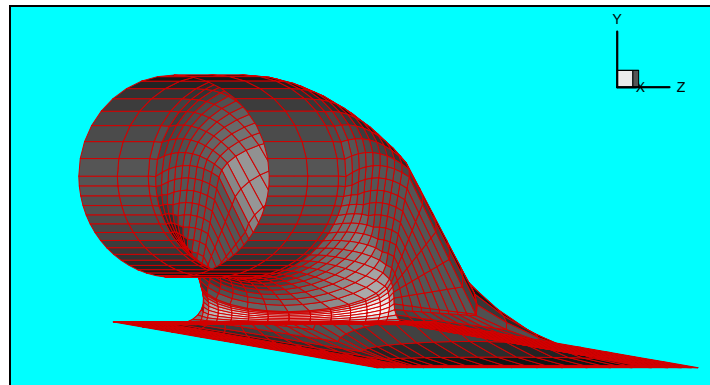


Figure 11: Waterjet Inlet Viewed from the Impeller Face End

## Nozzle Design

The nozzle is important in that it essentially loads the pump and will determine the pump operating point. Pump performance can be fine-tuned to its application by making appropriate small changes in the nozzle flow area to load the pump to its optimum condition once actual operational experience on a vessel is determined. The nozzle designs are typically of two types; a Pelton type or a parallel throat type. The Pelton type nozzle has converging walls, and the flow that exits the nozzle has some inward radial component of flow, which results in a Vena Contracta downstream of the nozzle exit where full thrust is determined. The Pelton nozzle is a minimum length, lighter weight arrangement that is more difficult to design in that the Vena Contracta must be determined to predict thrust, and it has a spray-like discharge beyond the Vena Contracta which can interfere with typical steering apparatus and would cause mixing associated losses for a submerged nozzle. The parallel throat nozzle has parallel walls at the nozzle exit, and the nozzle discharge is essentially free of any radial velocity component so that the waterjet full thrust occurs at the nozzle exit. The nozzle flow normally exits as a very uniform column of water with little, if any, spray until well aft of the ship. The parallel throat nozzle is somewhat longer than a Pelton type nozzle and would, therefore, have some weight disadvantage and some additional loss due to the additional length to turn the nozzle walls parallel. However, the cleaner flow will normally have less interference with the steering components when

these are not in use, and this type of nozzle will normally perform better for submerged applications as the clean flow is far less likely to induce mixing which can cause additional drag by inducing additional flow over adjacent portions of the hull. The stator blades were incorporated in the converging part of the parallel-throat-type nozzle section in order to minimize overall unit length and, therefore, reduce wet weight.

## PREDICTION OF PERFORMANCE AND CAVITATION LIMITS

The cavitation margin was set at 1.2 for a craft speed of 41 knots, which is 1.2 times the net positive suction head (NPSH) at complete pump head breakdown. The cavitation margin will allow the waterjet to absorb full installed power at 41 knots for acceleration to full speed and enhance off-design performance. The ram recovery,  $K_{ram}$ , is the percentage of the dynamic pressure at the pump face that remains from the amount that was in the inlet capture stream tube. The ram recovery is calculated from an empirical relationship that is a function of inlet velocity ratio, IVR, which is the ratio of average velocity at the pump face to the average velocity in the inlet capture stream tube. The ratio of the jet velocity from the nozzle to the ship speed is known as the jet velocity ratio (JVR). For a sealift type case, it was determined that a pump diameter of 90 inches would best meet cavitation and performance requirements for the 57,330 shaft horsepower. The jet velocity ratio (JVR) for this requirement is 1.56. A JVR in this range tends to provide the optimum balance between propulsive efficiency and unit size and weight.

The waterjet pump performance can be calculated from the ANSYS CFX calculations by summing up the tangential force on the rotor blade surface times their radius to calculate the required torque of the pump at the design RPM. The hydraulic power is calculated by taking the mass flow rate times the rise in total pressure across the pump. The pump hydraulic efficiency is the pump hydraulic power divided by the shaft power. Figure 12 shows the calculated pressure rise in feet of seawater versus flow rate in cubic feet per second. The optimum pump produces 4 percent more head than required at the design flow rate. Figure 13 shows the calculated shaft horsepower versus flow rate. Figure 14 shows the overall pump efficiency versus flow rate. The initial assumed design value of 90 percent is exceeded by 2.9 percent for the optimized pump. This higher efficiency can be used to push the ship faster using the 57,330 horsepower available, or represents a savings in fuel since less power will be needed to push the ship at 50 knots.

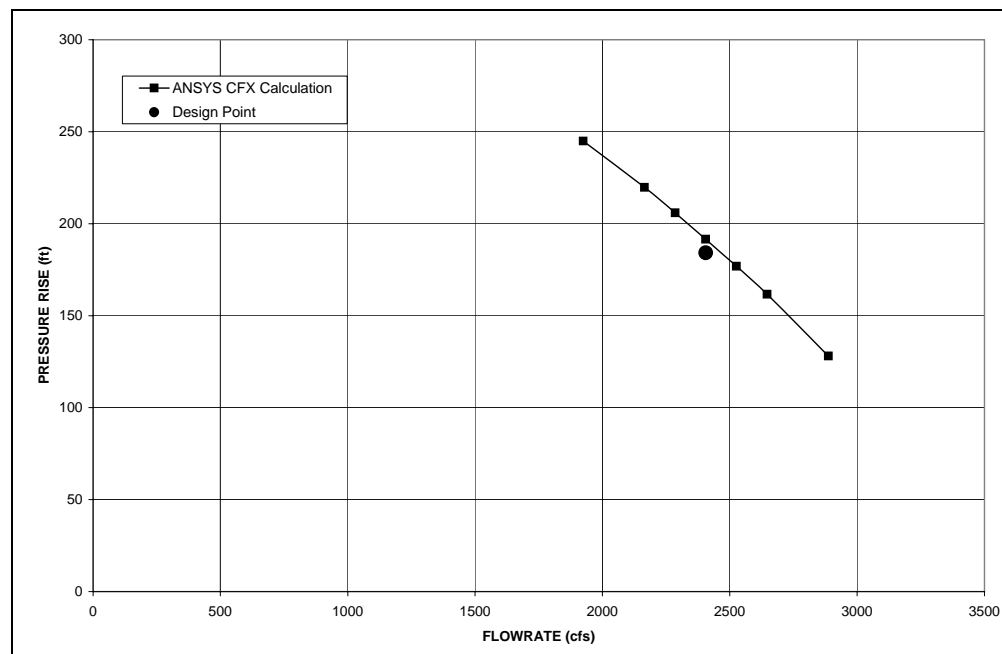
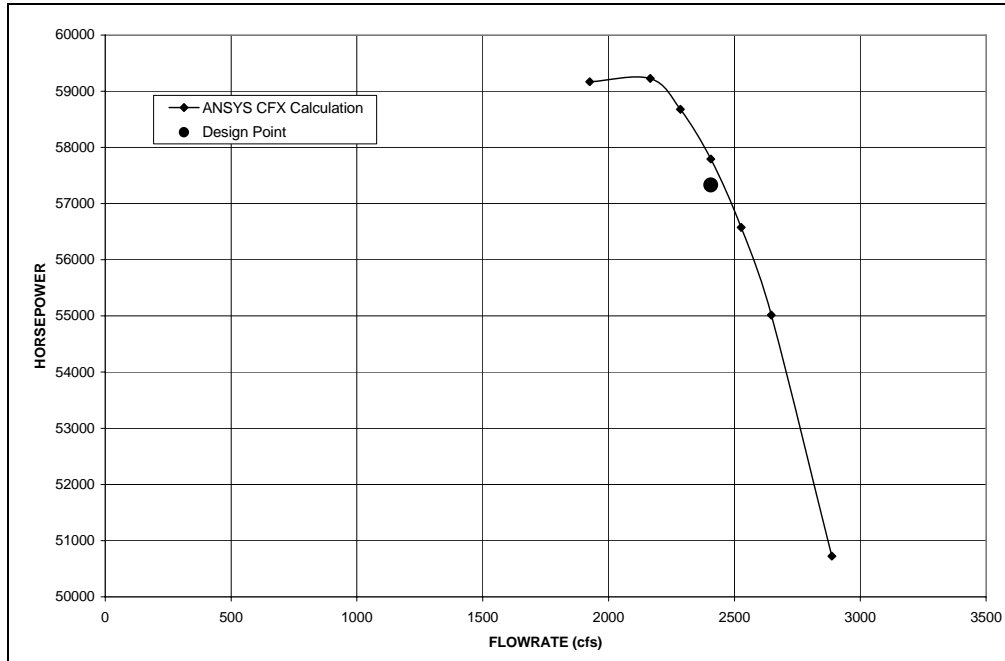
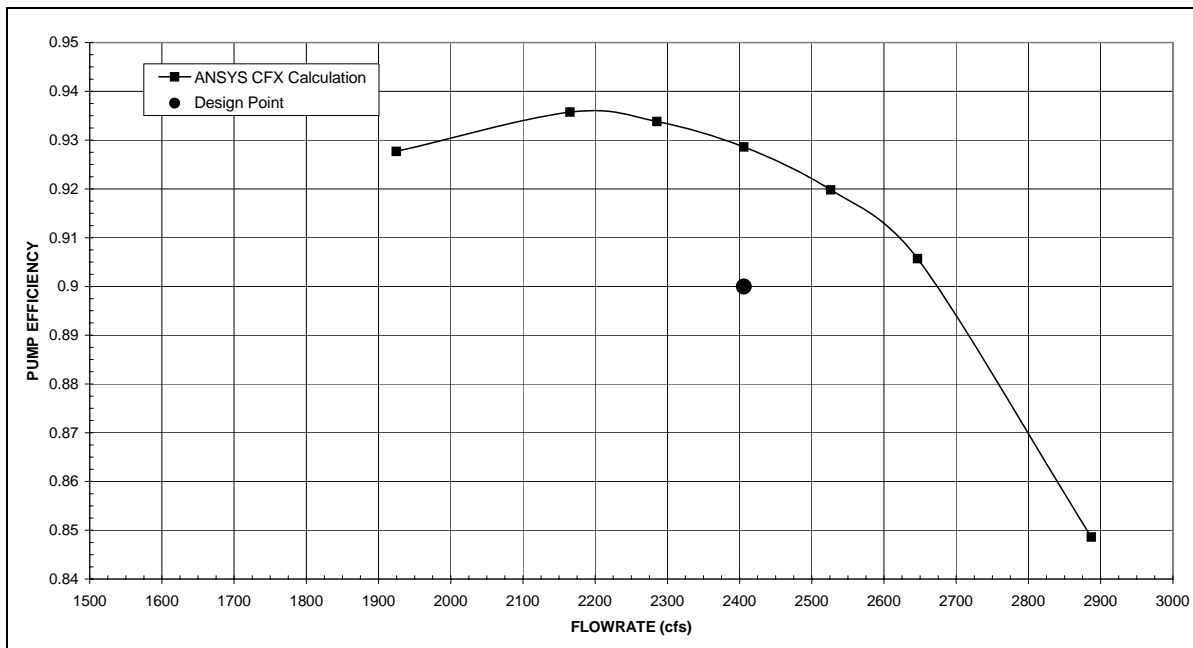


Figure 12: ANSYS CFX Calculated Head-Flow Curve



**Figure 13: ANSYS CFX Calculated Horsepower-Flow Curve**



**Figure 14: ANSYS CFX Calculated Efficiency-Flow Curve**

As a result of the CFD analysis of the overall design, several improvements to the initial design criteria were established. The ram recovery was higher than original empirical expectations. The large size of the waterjet inlet reduces its surface to volume ratio, which minimized frictional losses and improved the ram recovery from about 85 percent to near 90 percent. Increased ram recovery reduced the head rise requirements of the pump to operate at a given JVR and improved cavitation margins for the pump by increasing the NPSH. Stress analysis of the blading for the full-scale waterjet impeller and stator showed that stresses were well within reasonable limits for this design.

## MODEL TESTS

The water-tunnel testing of a 7.5-inch diameter pump, or 1/12<sup>th</sup>-scale model, of the advanced axial-flow waterjet pump was performed in the spring of 2005. Proper model testing requires proper construction of the model components, which requires special attention to details and quality machining. The water-tunnel testing was performed at the Carderock Division, Naval Surface Warfare Center (CDNSWC) in West Bethesda, MD, using the 24-inch water-tunnel facility. The water-tunnel pump model testing examined the performance and cavitation characteristics of a scaled axial-flow waterjet pump. The water-tunnel testing allows the basic full-scale pump performance to be evaluated from the use of the appropriately scaled model. The frontispiece of the technical paper shows a photo of the instrumented model axial pump assembly installed in the water tunnel and ready for testing. The water-tunnel testing allows the pump to be tested separately from the remainder of the waterjet system to determine its performance. Later self-propulsion tests of a suitable hull model with scaled waterjet inlets can then be conducted and later combined with the pump performance results to determine the overall waterjet system performance for the full-scale ship.

Model design point parameters:

Impeller diameter:	7.50 in
Nozzle diameter (unblocked):	4.87 in
Shaft speed (target):	2440 RPM
Shaft speed (acceptable):	2000 RPM
Maximum power:	50 SHP
Flow rate (target):	8.35 cfs
Headrise (target):	46 ft freshwater
Suction specific speed (design point):	12,730

Figures 15 and 16 show the schematic of the model test pump assembly and its water-tunnel installation. The water tunnel has a rear drive system, and the waterjet nozzle area was adjusted to account for the drive shaft blockage.

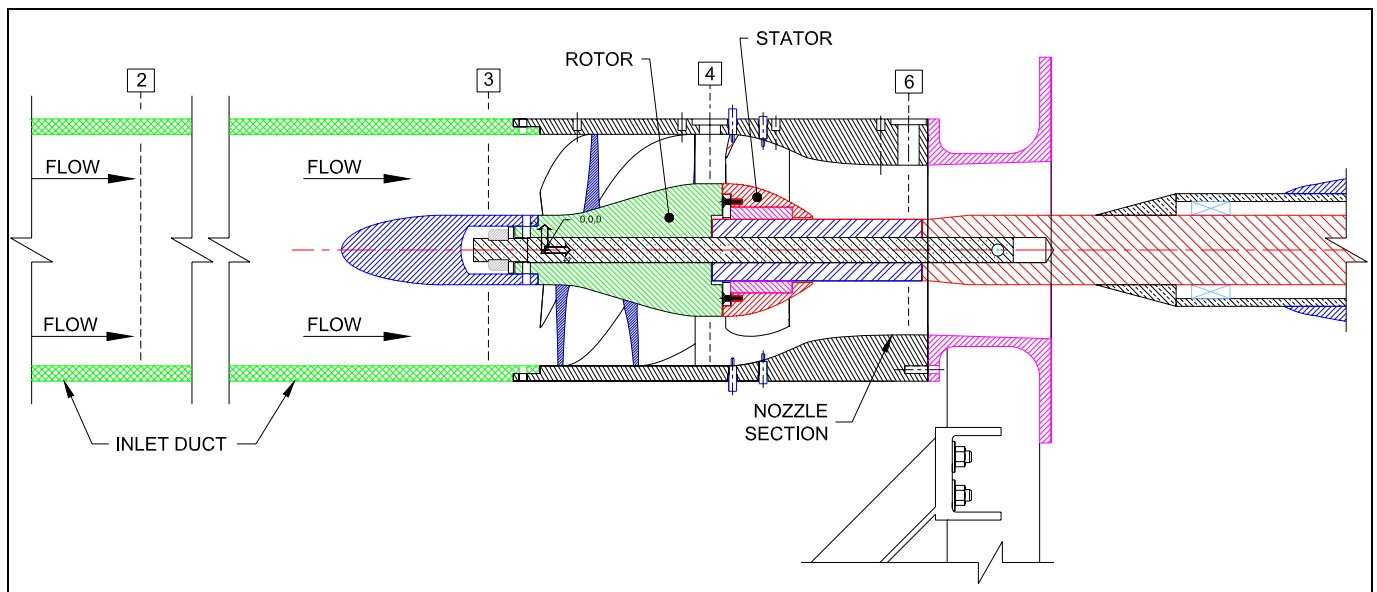


**Figure 15: Model Pump Assembly**

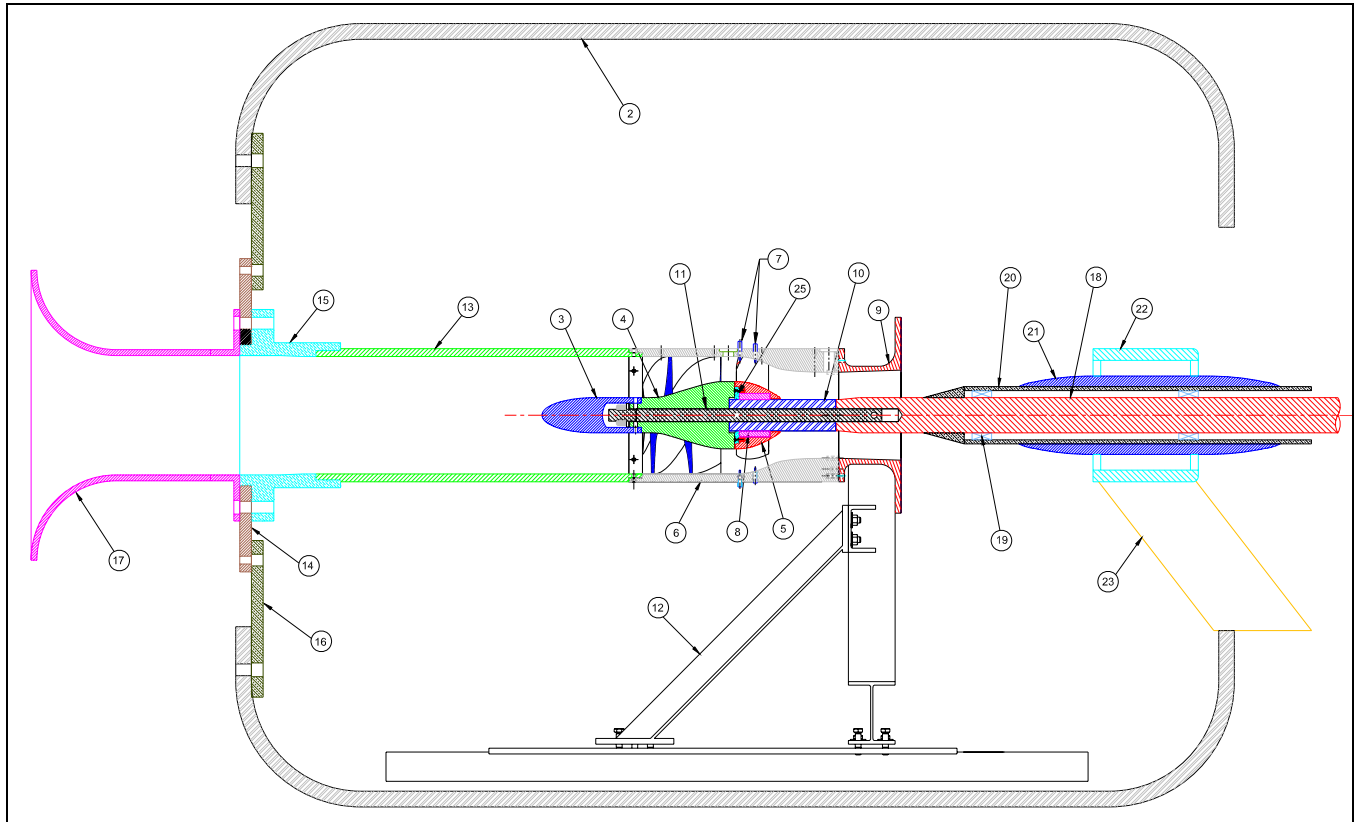


**Figure 16: Axial Pump Model Setup in the Water-Tunnel Test Section**

## **Pump Performance Tests**

Performance runs were made to ultimately establish the head-flow characteristics of the pump as well as its power requirements and hydraulic efficiency. These tests were run over a range of flows at different pump rotational speeds so that design and off-design conditions are covered. Various flow rates through the pump could be set by use of the tunnel circulation pump and/or additional flow resistance rods installed downstream of the pump exit nozzle. During the performance runs, multiple wall differential static pressure measurements were taken at locations between the pump inlet location and the rotor/stator gap and the nozzle throat. The wall static pressure differential gave information on the change in wall static pressures between locations and was supplemented with data from LDV surveys and Kiel probe data to generate the representative head-flow curve. All this data additionally determined the effective horsepower transmitted into the water by the pump impeller and what remains at the nozzle section so that rotor efficiency and overall pump hydraulic efficiency could be obtained at the various operating conditions. Figure 17 shows model performance data at 2000 rpm compared with initial CFD predictions for the model pump setup.

The water-tunnel drive motor was set up to measure the water-tunnel drive shaft torque. Corrections to torque were made to account for initial instrumentation offsets and drive system torque losses up to the pump using the tare test results. The resulting corrected torque values were the values of torque required to drive the pump rotor at its various test conditions.



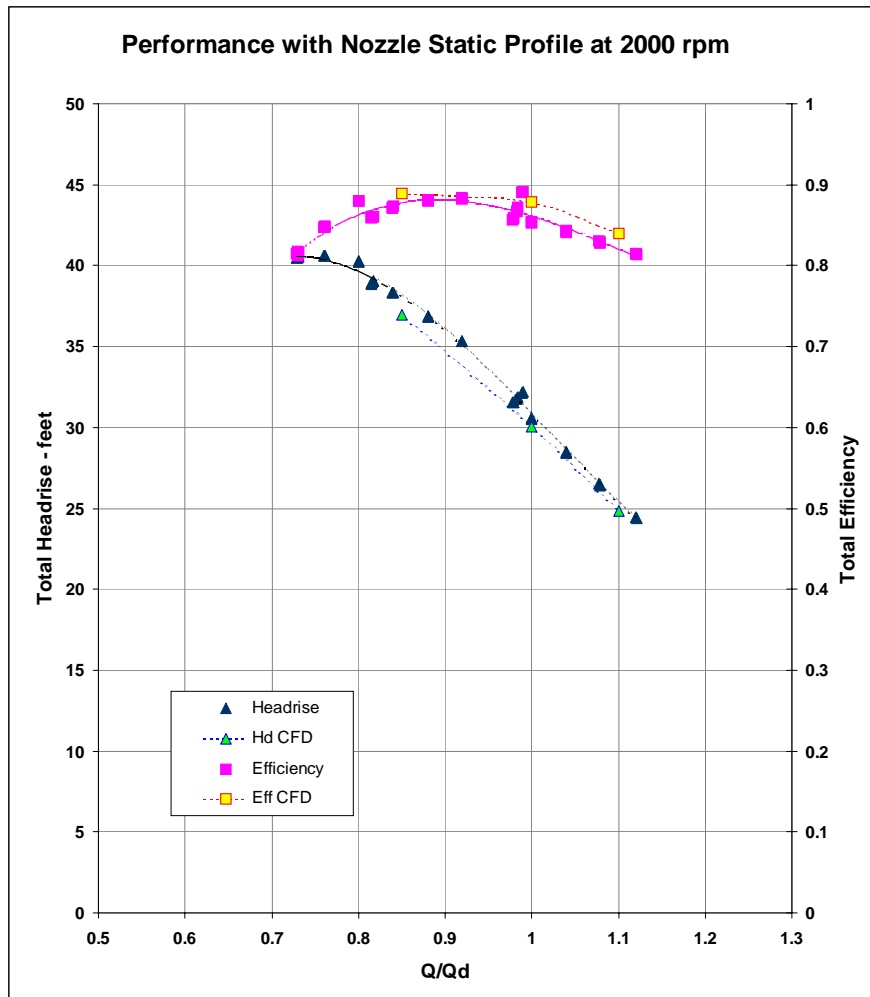


Figure 17: Performance with the Nozzle Static Profile at 2000 rpm

## Pump Cavitation Tests

Cavitation runs were made to determine the likely cavitation performance of the pump. During the cavitation runs, the tunnel pressure was changed to control the Net Positive Suction Head (NPSH) in front of the pump inlet face, where NPSH is the total pressure above vapor pressure at that location. The cavitation runs were performed at a test pump speed of 2000 rpm. The pump was mounted inside a clear acrylic shroud which enabled viewing of the impeller and stator blade rows as well as the nozzle section. By use of a strobe light, the rotating pump impeller could be made to appear as though it was standing still in order to observe any occurrences of cavitation in the impeller. In this manner, as the tunnel pressure was lowered sufficiently to initiate cavitation, the cavitation anywhere in the pump could be observed as to type, location and extent.

The presence of cavitation does not necessarily degrade performance, as a pump can operate with some amount of cavitation present. This is not desirable on a continuous basis, but is acceptable for transient operation such as during periods of ship forward acceleration. When the amount of cavitation present becomes excessive, the pump can no longer maintain its headrise and the pump enters cavitation breakdown where the headrise begins to fall off, usually in a dramatic form with any further decrease in NPSH. Cavitation breakdown is normally classified as the point where there is a 3% reduction in the pump total headrise from its noncavitating condition. Cavitation runs were made with decreasing NPSH until breakdown occurred, then the NPSH was increased to measure the recovery

from breakdown and to determine any hysteresis effects. Another term used for cavitation analysis is Suction Specific Speed (N<sub>ss</sub>). N<sub>ss</sub> is defined by:

$$N_{ss} = \frac{RPM * GPM^{1/2}}{NPSH^{3/4}} \quad [1]$$

N<sub>ss</sub> is a dimensionless term, but it is used with more convenient pump terms such as RPM and GPM, which makes it appear otherwise, but, since these terms only vary by a constant from the true dimensionless form, the N<sub>ss</sub> term functions as a dimensionless term. The N<sub>ss</sub> equation is important for scaling the model data to full scale since N<sub>ss</sub> performance at model scale will translate to the full-scale performance. Design point N<sub>ss</sub> for the full-scale design is about 12,500. The pump can operate at N<sub>ss</sub> values above this to provide for cavitation margins and better off-design performance, but operation at the elevated N<sub>ss</sub> should be kept to short periods, such as acceleration, as the increased presence of cavitation can damage the pump, although it may not affect performance until the breakdown N<sub>ss</sub> is reached. Design of a pump to operate properly with a high N<sub>ss</sub> of 12,500 or greater requires significant attention to the design detail. The use of CFD in the analysis has been a critical step in developing a high-performance design.

Figure 18 shows the cavitation run where the NPSH was changed in increments by adjustment of the tunnel pressure at the model design flow rate. The head ratio, H/H<sub>0</sub>, was the wall static pressure difference across the pump divided by the initial static pressure difference across the pump at the beginning of the test with a high NPSH value and no cavitation present. As the NPSH was reduced, the head ratio remained essentially constant at a value of 1 until a critical value of NPSH was reached, at which point a temporary increase in head ratio occurred prior to the collapse of the head ratio, which would indicate cavitation breakdown. This temporary increase in head ratio just prior to the breakdown region is not uncommon in cavitation testing and has been attributed to the existence of improved flow geometry due to a modest amount of cavitation. Figure 19 shows photos of the cavitation with increasing N<sub>ss</sub> (or decreasing NPSH) for the design flow case. Review of the photos indicates that the main source or type of cavitation that occurred was tip leakage cavitation. There is a pressure difference between the pressure and suction side of the blade. This pressure difference causes flow to accelerate through the tip gap between the rotating blade tip and the surrounding stationary shroud. Some flow through the gap is beneficial, but an increase in pressure difference across the gap, combined with the local pressure conditions, can cause the flow accelerating through the gap to drop the local static pressure below the vapor pressure, which results in the formation of a jet of vapor. The photos also indicate that the tip leakage was not always uniform from blade to blade at different N<sub>ss</sub> values. This was most likely due to tip clearance variations from blade to blade. Although every attempt was made to center the impeller in the shroud, the small scale of the model, the final component assembly after the gap is set, and operating loads inevitably caused some minor variations in the gap.

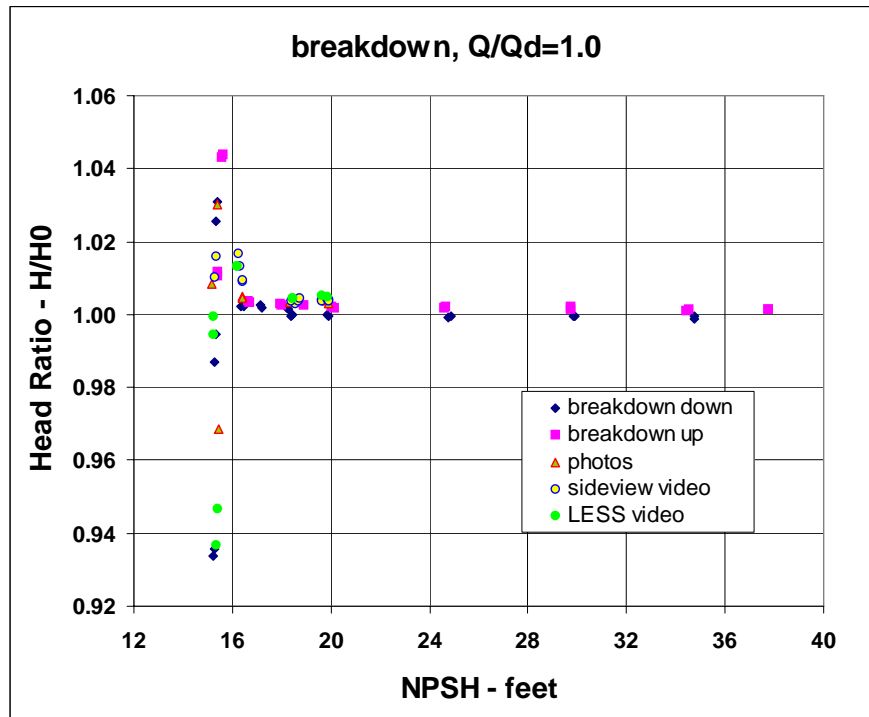
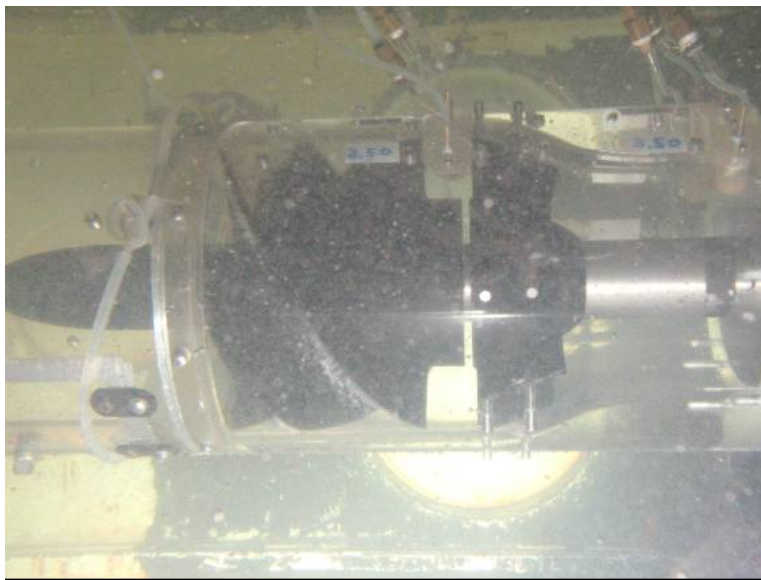
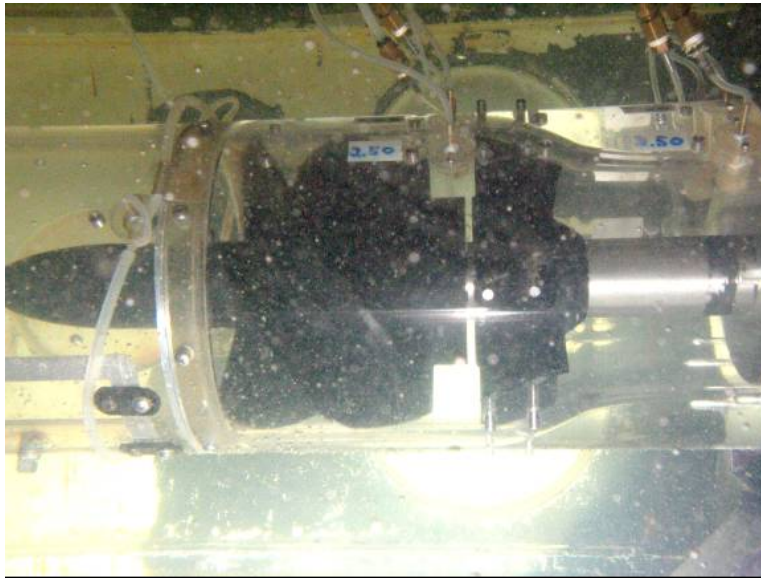


Figure 18: Cavitation Breakdown Runs at  $Q/Q_d = 1.0$  and 2000 rpm





**Figure 19: Cavitation Runs at 2000 rpm and  $Q/Q_d = 1.0$   
Suction Specific Speed (top to bottom) = 12,500, 13,588, and 14,395**

The tip leakage cavitation can be controlled to some extent to allow operation of the full-scale pump at higher  $N_{ss}$  values. Better control of the tip clearance to optimum values will delay the onset of cavitation. Also, the model pump had sharp corners at the impeller tip section. Putting a small radius on the pressure side tip section will enable a more gradual acceleration of flow through the tip gap instead of the abrupt acceleration caused by the square edge arrangement. This would help push the tip leakage cavitation inception to somewhat higher  $N_{ss}$  values. In addition, the model likely experienced a higher differential pressure across the tip gap due to an increased amount of boundary layer flow that was present at the pump face from the test setup. The photos indicate that the impeller leading edge is not a source of cavitation and there is no indication of cavitation problems in the stator or nozzle region. The S-bend in the shroud wall shortly after the stator exit is a typical low-pressure region, but did not show any indication of vapor formation.

### **Self-Propelled Model Tests**

CDIM-SDD has conducted extensive advanced axial-flow waterjet propulsion work, and the upcoming self-propelled model tests represent the completion of a four-phase program for CCDoTT to develop an advanced axial-flow waterjet propulsor for high-speed sealift application where waterjet propulsion is the only realistic choice. Axial-flow waterjets are an enabling technology for the weight-sensitive, slender hulls of high-speed ships. This is as a result of the pumps' much lower weight and their much narrower installation requirement, which allows the multiple units that are typically required to be installed without compromising the geometry of the slender high-speed hulls, compared to the commercially available large waterjets which use a wider, heavier mixed-flow impeller arrangement. The overall objective of the final phase of work is to test a self-propelled model in a towing tank to completely define the hydrodynamic performance characteristics of an advanced-design axial-flow waterjet propulsor in a representative high-speed ship. Measurements will be used to verify design predictions, provide off-design performance information, and yield flow-field data for use in understanding the behavior of the propulsion system design as installed in the hull model. Data will ultimately be scaled to the full-scale ship design used for the model, using the waterjet design which was water-tunnel model tested, and that data combined with this self-propulsion model will be used to predict performance of an operational system at full scale. Towing tank tests of waterjet propulsors and ship hulls present a unique challenge to engineers and experimenters because of interaction effects normally absent, or of far less importance, in marine-screw propeller installations. The great body of towed model test data and experience with open propeller designs has resulted in a generally high degree of confidence in predicting full-scale performance. Waterjet hull model testing is relatively new, and the body of test data and testing experience is a small fraction of the propeller database. For these reasons, the fundamentals of waterjet model

testing have been the subject of a great deal of attention and study in recent years. The development of the momentum flux method of estimating powering characteristics and interaction effects has allowed model testing to be performed with better confidence than previously, and the database is expanding slowly but steadily. While the overall waterjet characterization capabilities remain somewhat limited relative to open water and towed model propeller testing, prediction techniques are improving. The development of a database with a significant quantity of model to full-scale data correlations is a matter of great importance in improving levels of confidence in predicting waterjet system performance for advanced high-speed ships.

## **CONCLUSIONS**

The advanced axial-flow waterjet pump model has demonstrated generally excellent overall hydrodynamic and cavitation characteristics. Performance of the pump is basically in agreement with initial CFD predictions, although some differences between the CFD pump model details and the actual test setup are responsible for certain variations. Overall headrise was slightly higher than expected, but this is likely due to the thick duct wall boundary layer flow region upstream of the model impeller. Efficiencies were slightly lower than CFD predictions, but the differences between the CFD arrangement and the model test geometries mentioned are deemed likely to account for most of the variation. Further analyses would be incorporated into the development and adaptation of the advanced axial-flow pump design as a matter of course to refine the design.

## **ACKNOWLEDGEMENTS**

Assisting CDIM-SDD in Severna Park, MD, on this project for CCDoTT has been the Naval Surface Warfare Center, Carderock, MD (NSWCCD), Marine Propulsors Company, Berlin, MD (MPC), and the Office of Naval Research (ONR).

Specific individuals that have made significant contributions to this four-year program of work, and for which we are very grateful, have included: Alan Becnel (CDIM-SDD and NSWCCD); John Stricker (MPC); Scott Gowing (NSWCCD); Diane King and Bill Baker (CDIM-SDD); Stan Wheatley and Steve Hinds (CCDoTT); Dan Sheridan (Noesis); and Dr. Ki-Han Kim and Dr. Paul Rispin (ONR).

## **REFERENCES**

ALLISON, J.L. "Marine Waterjet Propulsion." *Transactions* of SNAME, 101 (1993).

NSWCCD-20-TR-2002/06. "High-Speed Sealift Technology Development Plan." (May 2002).

PROCEEDINGS OF THE 23<sup>RD</sup> ITTC – VOLUME II. "The Specialist Committee on Validation of Waterjet Test Procedures." Final Report and Recommendations to the 23<sup>rd</sup> ITTC, p 387-415, p 709-711. (2002).